Liquid Crystals
Publication details, including instructions for authors and subscription information:
http://www.informaworld.com/smpp/title~content=t713926090

Order parameters of the mesogenic core in two nematic liquid crystals containing a four-unit link

J. -P. Bayle[a]; B. M. Fung[b]
[a] Laboratoire de Chimie Structurale Organique, Orsay, Cedex, France [b] Department of Chemistry and Biochemistry, University of Oklahoma, Norman, Oklahoma, U.S.A.

To cite this Article Bayle, J. -P. and Fung, B. M.(1993) 'Order parameters of the mesogenic core in two nematic liquid crystals containing a four-unit link', Liquid Crystals, 15: 1, 87 — 102
To link to this Article: DOI: 10.1080/02678299308027841
URL: http://dx.doi.org/10.1080/02678299308027841

LIQUID CRYSTALS, 1993, VOL. 15, NO. 1, 87–102

Order parameters of the mesogenic core in two nematic liquid crystals containing a four-unit link

by J.-P. BAYLE
Laboratoire de Chimie Structurale Organique,
Batiment 410, Université Paris XI, Orsay Cedex, 91405, France

and B. M. FUNG*
Department of Chemistry and Biochemistry,
University of Oklahoma, Norman, Oklahoma 73019-03079, U.S.A.

(Received 28 August 1992; accepted 16 February 1993)

A series of compounds containing a four-unit link, 4′-*n*-alkylphenyl-4-*n*-hexyloxycinnamates, has been synthesized, and their mesomorphic behaviour has been determined. The orientational ordering of two compounds in this series has been studied in detail by 2D carbon-13 nuclear magnetic resonance with variable angle sample spinning. The carbon-proton dipolar coupling constants were obtained and the order parameters were calculated for different molecular segments (two phenyl rings, the central link containing an ethylenic motif, and the methylene carbons of the alkoxy chain). The temperature dependence of the local order parameters of each fragment were determined using these data and C-13 chemical shifts which were measured as a function of temperature. In these non-rigid molecules, the ratio between the order parameters of the two phenyl rings was found to be temperature dependent. The ring bearing the double bond is more ordered at low temperatures compared to the ring bearing the short alkyl chain, but this behaviour is reversed near the clearing point. The position of the major axis of the rigid core was calculated from the order parameter of one ring and the order parameter of the ethylenic link. It was found that this major axis forms a constant angle with respect to the *para* axis of the phenyl ring connected to the ethylenic group. On the other hand, the angle of this major axis with respect to the *para* axis of the phenyl ring connected to the carboxylic group is temperature dependent, varying from 11° at $T/T_{NI}=0{\cdot}92$ to 7° at $T/T_{NI}=0{\cdot}98$.

1. Introduction

Nematic liquid crystals are anisotropic fluids which possess a unique feature of being oriented in a magnetic or an electrical field. This molecular arrangment of molecules can be described by the averaged position of the long axis of the mesogenic unit (major axis of the rigid core) with respect to the external field and by the order parameters of the mesogen fragments. These local order parameters can be experimentally studied by NMR spectroscopy [1]. The 2D method of variable angle spinning combined with separated local field spectroscopy (VAS/SLF) has been proven to be very successful in the determination of the local ordering parameters by C-13 NMR [2–14]. So far, only liquid crystals with a linkage containing 0 and 2 atoms have been studied by this method. Molecular ordering has been obtained for some 4-*n*-alkyl(alkyloxy)-4′-cyanobiphenyls [3–6], phenylcyclohexanes [6, 7], bicyclohexylnitriles [8, 11], chiral liquid crystals [9, 10, 12], 4′-cyanophenyl-4-

---

* Author for correspondence

alkylbenzoates [15] and Schiff bases [16]. In these compounds the molecular ordering was determined for the rings as well as the terminal chains. Due to the effective D_2 symmetry of each phenyl ring, the VAS/SLF experiment gives two non-zero values of the order parameters, S_{zz} and S_{xx}-S_{yy}, where the z axis is the C_2 axis of the ring and the y axis is normal to the ring. However, the C_2 axes of the two rings are not always collinear, and the position of the major axis of the rigid core cannot be easily determined from the values of the order parameters of the two rings. On the other hand, by choosing a four-unit link containing two protonated ethylenic carbons, the position of the major axis of the rigid core in the molecular frame can be determined from the dipolar couplings of the linking segment. In this paper, we present the synthesis of some nematic liquid crystals containing a cinnamic ester link and the results of the orientational ordering study of two of these compounds.

2. Experimental

The synthesis of the cinnamic esters are shown in the scheme.

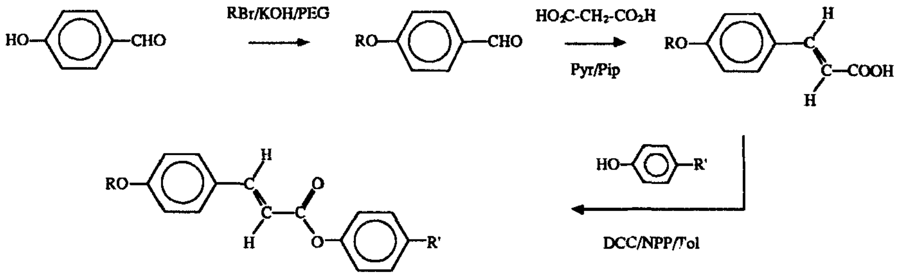

The synthesis of 4′-alkylphenyl-4-alkoxycinnamate.

4-*n*-Alkoxybenzaldehydes and *trans*-4-*n*-alkoxycinnamic acids were synthesized according to procedures described elsewhere [17]. The esters 4′-*n*-alkylphenyl-4-*n*-alkoxycinnamates were prepared by boiling a mixture of 4-*n*-alkoxycinnamic acid (0·01 mol), 4-*n*-alkylphenol (0·011 mol), 1,3-dicyclohexylcarbodiimide (0·011 mol) and 4-pyrrolidinopyridine (0·001 mol) in dry toluene (20 ml) for 2 h. The mixture was then allowed to cool down to room temperature. The 1,3-dicyclohexylcarbodiimide hydrate was filtered and the organic phase was washed twice with water (50 ml), twice with 5 per cent acetic acid solution (50 ml) and three times with water (50 ml). The organic phase was dried over sodium sulphate and alter filtration 95 per cent ethanol was added at room temperature (50 ml). The solution was left at room temperature until complete crystallization of the ester occurred. Then the compound was recrystallized in a mixture of toluene/ethanol/4-methyl-2-pentanone (25/65/10) until constant transition points were obtained.

The purity of the compounds was monitored by thin layer chromatography (TLC). The phase transitions were observed by the use of an Olympus BHT polarising microscope fitted with a Linkam PR600 heating stage, and by the use of a Perkin-Elmer DSC-2 differential scanning calorimeter.

The 2D SLF/VAS C-13 NMR experiments were performed using a Varian XL-300 NMR spectrometer at $B_0 = 7{\cdot}05$ T. The angle between the spinning axis and the magnetic field was set at *c.* 48°. The exact value of the angle was determined for each experiment by measuring the ratio of the F–F dipolar coupling of 2,2-difluoro-1,1,1,2-tetrachloroethane dissolved in the nematic phase of ZLI 1291 with and without sample spinning. Temperature calibration was performed by observing the nematic to isotropic phase transition. The data from the XL-300 NMR spectrometer was processed on a VXR-4000 data station.

The C-13 chemical shifts were obtained on a Varian VXR-500 NMR spectrometer at 11·70 T. The sample was put in a standard NMR tube and the sample height was only about 1·5 cm to minimize the temperature gradient in the sample. To avoid radiofrequency (RF) overheating a 0·7 per cent decoupler duty cycle was used. The temperature calibration was again made by observing the nematic to isotropic transition.

3. Results and discussion

3.1. *Transition temperatures*

Twelve 4′-alkylphenyl-4-alkoxycinnamates were synthesized and their transition temperatures were determined. Compounds in homologous series I are 4′-methylbenzyl-4-*n*-alkoxycinnamates. The transition temperatures of five compounds in this homologous series are given in table 1. All of the compounds are monotropic liquid crystals with the exception of those with C6 and C8 terminal chains. The nematic phase shows a threaded texture when it is the only phase encountered (for $n=4$ and 5), but it becomes homeotropic for compounds with a smectic phase as well ($n=6$, 7, 8). The smectic phase displays a focal-conic fan shaped texture typical for a smectic A phase.

Figure 1 shows the dependence of the transition temperatures on the number of atoms, *n*, in the terminal alkoxy chain. The most prominent feature is the increase in the smectic A phase temperature range with the number of carbons in the terminal chain. In fact, it has been observed that a four unit linkage conjugated like –CH=CH–COO– enhances the smectic phase [18]. Usually, the nematic phase has a narrow range, and the compounds are in general strongly monotropic.

In order to examine the effect of both the alkyl chain and the alkoxy chain on the phase behaviour, we have synthesized two other series of compounds with short alkoxy chains containing 4 and 6 carbons, namely the 4′-*n*-alkylbenzyl-4-butoxycinnamates (series II) and the 4′-*n*-alkylbenzyl–4-hexyloxycinnamates (series

Table 1. Transition temperatures (in °C) of series I. Values in parentheses are taken with decreasing temperature.

n	C	→	S_A	→	N	→	I
4	●	122·9					●
	●	(60·8)			●	(106·6)	●
5	●	102·0					●
	●	(72·9)			●	(98·1)	●
6	●	93·9			●	103·4	●
	●	(60·1)	●	(66·6)	●	(103·3)	●
7	●	104·3					●
	●	(57·0)	●	(71·2)	●	(97·2)	●
8	●	96·9			●	100·6	●
	●	(61·9)	●	(81·4)	●	(100·4)	●

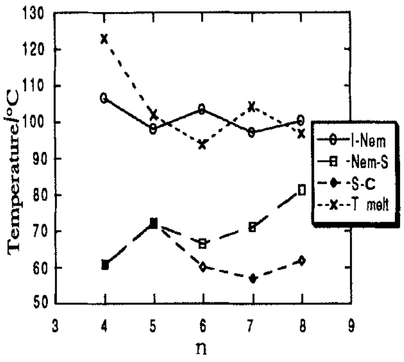

Figure 1. Phase behaviour for the homologous series I. *n* is the number of carbons in the alkoxy chain. The transition temperatures (cooling) were obtained by optical measurements.

Table 2. Transition temperatures (in °C) of series II. Values in parentheses are taken with decreasing temperature.

n	C	→	N	→	I
1	●	122·9			●
	●	(60·8)	●	(106·6)	●
3	●	98·3	●	111·7	●
	●	(74·8)	●	(111·4)	●
5	●	104·8	●	114·1	●
	●	(69·4)	●	(113·9)	●

III). The transition temperatures of the compounds in these series are given in tables 2 and 3, respectively.

All the compounds are enantiotropic nematogens with the exception of the first member of series II. Figure 2 shows the dependence of the transition temperatures on the length of the terminal alkyl chains for both series. No smectic phase is

Table 3. Transition temperatures (in °C) of series III. Values in parentheses are taken with decreasing temperature.

n	C	→	S_A	→	N	→	I
1	●	93·9			●	103·4	●
	●	(60·1)	●	(66·6)	●	(103·3)	●
2	●	80·8			●	98·7	●
	●	(61·9)	●	(70·8)	●	(98·5)	●
3	●	89·9			●	110·8	●
	●	(64·9)	●	(78·8)	●	(110·7)	●
5	●	90·4			●	110·2	●
	●	(66·3)	●	(89·8)	●	(110·1)	●

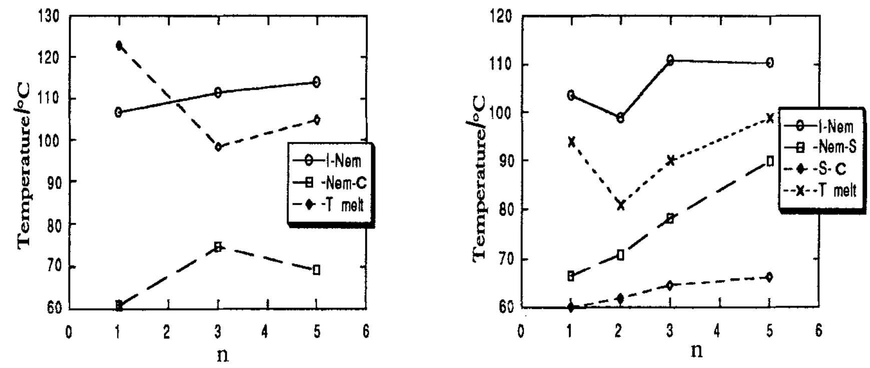

Figure 2. Phase behaviour for the homologous series II and III. *n* is the number of carbons in the alkyl chain. The transition temperatures (cooling) were obtained by optical measurements.

observed for series II. A smectic A phase is present for all the members of series III, and its range increases progressively with the number of carbons in the terminal chain.

In order to have reasonable melting points and a sufficiently large nematic range, we have chosen two compounds in series III with $n=1$ and $n=2$ to perform the 2D SLF/VAS experiments which are labelled, respectively, Cin-6-1 and Cin-6-2.

3.2. *Order parameters of the phenyl rings*

The dipolar coupling constants for individual bonded or non-bonded C,H pairs were calculated from the splittings obtained in the ω_1 dimension of the 2D-SLF/VAS experiment. Figures 3 (*a*) and (*b*) show C-13 spectra for the aromatic and aliphatic regions of 4′-methylbenzyl-4-hexyloxycinnamate at 80°C. In the aromatic region, all peaks are resolved with the exception of carbon 6, which overlaps with the peak belonging to carbon 2. In the aliphatic region, all the peaks are resolved.

Spectra in the ω_1 dimension are displayed in the upper part of figures 3 (*a*) and (*b*). These figures show first order C–H couplings. The type of the pattern is indicated by a capital letter above each trace. D, T, Q refer to doublet, triplet, and quartet, respectively.

For the main core of the molecule, three distinct parts can be defined, which include the two phenyl rings and the central link. Thus, we can obtain from the experiments the ordering matrices for individual sub-units with respect to their molecular frames defined in figure 4.

The phenyl rings undergo rapid jumps about their *para* axis, inducing an equivalence between the two *ortho* and the two *meta* positions. Then, for each of the protonated aromatic carbons, the pattern in the second dimension is a doublet of doublets due to the splitting of the directly bonded proton and the *ortho* proton (see figure 3 (*a*)). The doublet of doublets for carbons 3 and 10 are broadened due to unresolved couplings with H5 and the alkyl protons, respectively. Carbon 1 appears as a triplet due to splittings with protons 2 and 2′, and the same pattern is observed for carbon 8 coupled with hydrogens 9 and 9′. Carbon 4 is a doublet of triplets caused by couplings with hydrogens 3, 3′ and 5. Carbon 11 is a quartet of triplets due to the couplings with hydrogens 10, 10′ and hydrogens in the terminal methyl group.

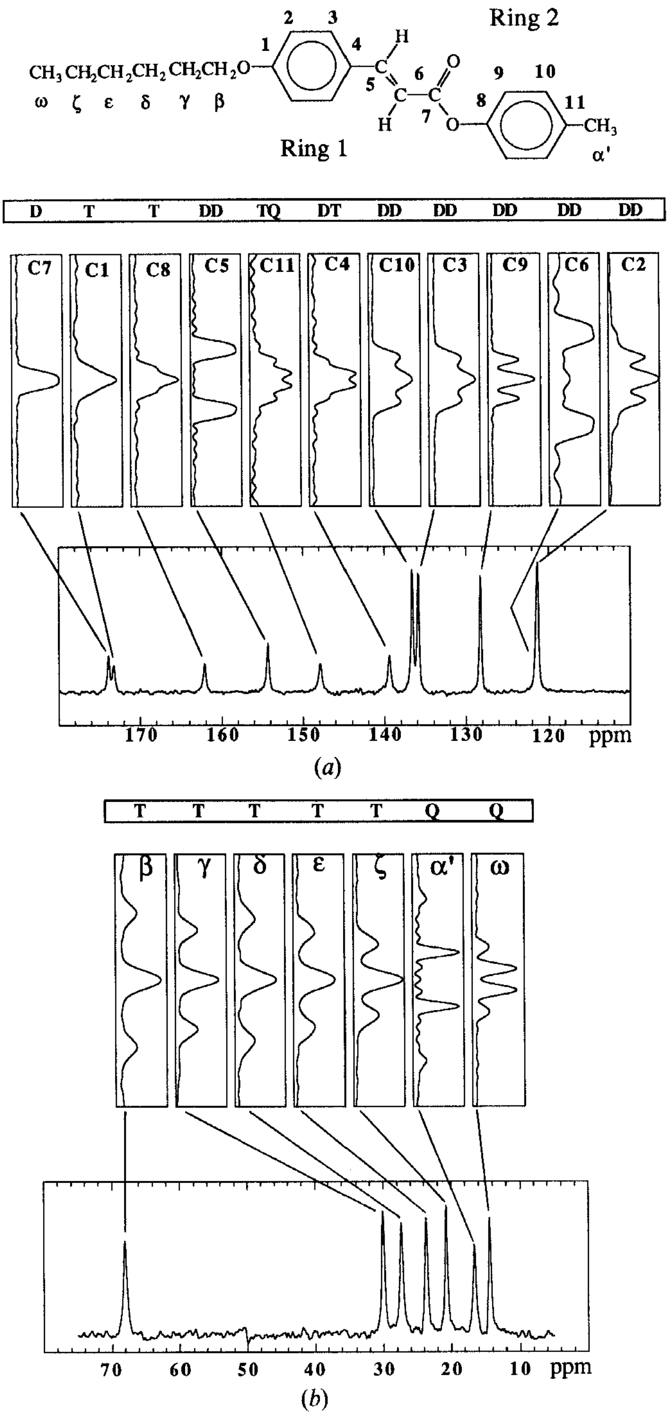

Figure 3. Carbon-13 spectra of Cin-6-1 at 75·4 MHz and $T = 80°C$. (*a*) Aromatic part. (*b*) Aliphatic part. The spectra were obtained by the VAS/SLF method. The parameters used in this experiment are $\theta = 48{\cdot}3°$, spinning rate 1·0 kHz and a decoupling field of 21·8 kHz. Spectra in the ω_1 dimension are shown on the top, the spectral width is 3000 Hz. The first spectrum in the ω_2 dimension is shown at the bottom. The type of the pattern of each trace is given above each trace.

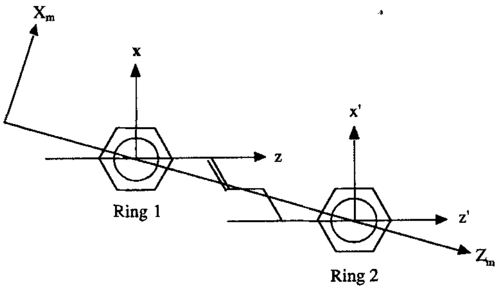

Figure 4. Different frames in which the local ordering matrices for individual sub-units are determined.

Since most of the signals are overlapping multiplets, the splittings were obtained by numerical lineshape fitting [2–14]. Then, the dipolar couplings constants can be obtained from the equation

$$\Delta \nu = f[(3\cos^2\theta - 1)D + J]. \tag{1}$$

where f is the scaling factor characteristic of the dipolar decoupling sequence (0·42 for BLEW-48 sequence), θ is the angle between the spinning axis and the magnetic field, and J is the C–H scalar coupling constant determined from the isotropic coupled C-13 spectrum. The experimental error in the absolute value of the dipolar couplings is estimated at 5 per cent. The order parameters of the phenyl rings were calculated with a standard procedure using the dipolar coupling constants [2–14]. In the first step of the calculation the C–C–H aromatic bond angles were treated as variables at every temperature for each compound. To refine the calculation the average value of each C–C–H aromatic bond angle was treated as a constant. With the exception of the H9–C9–H10 angle, these values are close to the undistorted angle of 120° (see table 4). The unusually large value of the H9–C9–H10 bond angle may be attributed to enhanced van der Waals attraction between the slightly acidic hydrogen (as bonded to a sp^2 carbon) and the oxygen of the neighbouring carbonyl group which is quite electronegative due to the extended conjugation with the aromatic ring [15]. The values of the order parameters of the phenyl rings in the two compounds studied are given in table 5, where the x axis is in the plane of the phenyl ring and perpendicular to the z axis, and the normal to the ring is defined as the y axis. The relatively large values of S_{zz} and $S_{z'z'}$ compared to other compounds studied may be due to the extension of the rigid core by the four-atom link with a double bond. A strong lateral dipolar group (like the carbonyl

Table 4. Average values of H–C–C angles for the aromatic rings found by the VAS/SLF method.

Angle	Value
H2–C2–C3	120·2° ± 0·3°
C2–C3–H3	119·8° ± 0·3°
H9–C9–C10	121·8° ± 0·3°
C9–C10–H10	120·4° ± 0·3°

Table 5. Order parameters for the aromatic rings at different values of T/T_{NI} for Cin-6-1 and Cin-6-2. These values were obtained from the dipolar couplings using the C–C–H angles listed in table 4.

Cin-6-1	Ring 1		Ring 2	
T/T_{NI}	S_{zz}	S_{xx}-S_{yy}	$S_{z'z'}$	$S_{x'x'}$-$S_{y'y'}$
0·928	0·679	0·034	0·662	−0·011
0·934	0·675	0·043	0·658	−0·017
0·940	0·662	0·039	0·647	−0·003
0·945	0·655	0·037	0·640	−0·006
0·955	0·624	0·046	0·626	−0·004
0·965	0·608	0·033	0·609	−0·009
0·978	0·577	0·032	0·593	−0·004

Cin-6-2	Ring 1		Ring 2	
T/T_{NI}	S_{zz}	S_{xx}-S_{yy}	$S_{z'z'}$	$S_{x'x'}$-$S_{y'y'}$
0·927	0·679	0·027	0·661	−0·005
0·940	0·649	0·021	0·642	−0·006
0·952	0·621	0·016	0·625	−0·006
0·968	0·603	0·019	0·610	−0·006
0·977	0·588	0·019	0·583	−0·004

group in the link) may favour the more ordered smectic phase, which often has large order parameters persisting close to the isotropic phase. It may be the reason why four-atom conjugated link liquid crystals easily form smectic phases if the terminal alkyl/alkoxy chains are sufficiently long [18].

It has been shown that the chemical shift changes obey the semi-empirical equation [14]

$$\delta_{obs} - \delta_{iso} = a \cdot S_{zz} + b, \qquad (2)$$

where a and b are constants which are assumed to be independent of temperature within experimental error. Usually $a \gg b$, and $a \approx (2/3)[\sigma_{zz} - (\sigma_{xx} + \sigma_{yy})/2]$ for the aromatic carbons. The constants a and b can be determined from several measurements of S_{zz} at different temperatures. If it is assumed that in a homologous series the number of carbons in the terminal alkyl chain does not change the chemical shift anisotropy tensor values of the aromatic carbons, data for different compounds in the same series can be pooled. In figure 5, the anisotropic chemical shifts of the two compounds are plotted versus the order parameters obtained by the VAS/SLF method. A single linear relation is observed for each carbon in both compounds, except for C11. This carbon is substituted by a methyl group in Cin-6-1 and by an ethyl group in Cin-6-2. Although a substituent affects the C-13 shielding tensor of every carbon in the benzene ring, its effect is mainly localized on the carbon at which the substitution occurs [20], namely the C11 carbon in our case. The C-13 chemical shift tensors of alkyl substituted carbons for toluene, durene, hexamethylbenzene, hexaethylbenzene are known [20] and give a chemical shift anisotropy of 182, 174, 169, 171 ppm, respectively. These values can be compared to the values of $3a/2 = 155$ and 171 ppm for C11 in Cin-6-1 and Cin-6-2, respectively. This explains why the two lines are nearly parallel, but the position of each line is determined by the constant *b* which is approximatively equal to $(S_{xx}\text{-}S_{yy})(\sigma_{xx}\text{-}\sigma_{yy})$. The values of $S_{xx}\text{-}S_{yy}$ are very small (see table 5) and not sufficiently accurate for the determination of $\sigma_{xx}\text{-}\sigma_{yy}$ from *b*. On the other hand, if it is assumed that $S_{xx}\text{-}S_{yy}$ is nearly equal for the two compounds, the positions of the lines depend on the values of $\sigma_{xx}\text{-}\sigma_{yy}$. For the aromatic carbons in hexamethylbenzene and hexaethylbenzene, these values are -78 ppm and -56 ppm, respectively [20]. Because the biaxiality component $S_{xx}\text{-}S_{yy}$ is negative (see table 5), the value of *b* with a CH_3 substituent should be larger than that with a C_2H_5 substituent for the cinnamates. This can explain that in figure 5 the line corresponding to the methyl substituted compound (labelled C11-1) is above the line corresponding to the ethyl substituted compound (labelled C11-2).

From the *a* and *b* values obtained for each carbon, the values of *S* can be calculated from the chemical shift. This allows a large amount of data to be obtained, which tends to moderate the uncertainties of S_{zz} measurements by the VAS/SLF method. The temperature dependence of these data can be fitted using the empirical formula [21]

$$S(T)=S_0(1-T/T_{\mathrm{NI}})^F. \qquad (3)$$

The best fit is represented by the dashed line in figure 6, and the S_0 and *F* values obtained from the least square fit are listed in table 6.

It should be pointed out that equation (3) is an empirical rather than a theoretical equation, and is not strictly valid near the clearing temperature [21]. However, the physical meaning of the parameters S_0 or *F* are quite simple: S_0 should be the limit of the order parameter with decreasing temperature and *F* may be considered as an indication of how quickly a molecular fragment reaches the limit of the order parameter as a function of change in temperature. A comparision of these values is relevant as they are obtained in the same set of experiments and encounter the same experimental errors. Because the first ring is linked to a very conjugative group and the second ring is linked to an ester group, which is not conjugative, the

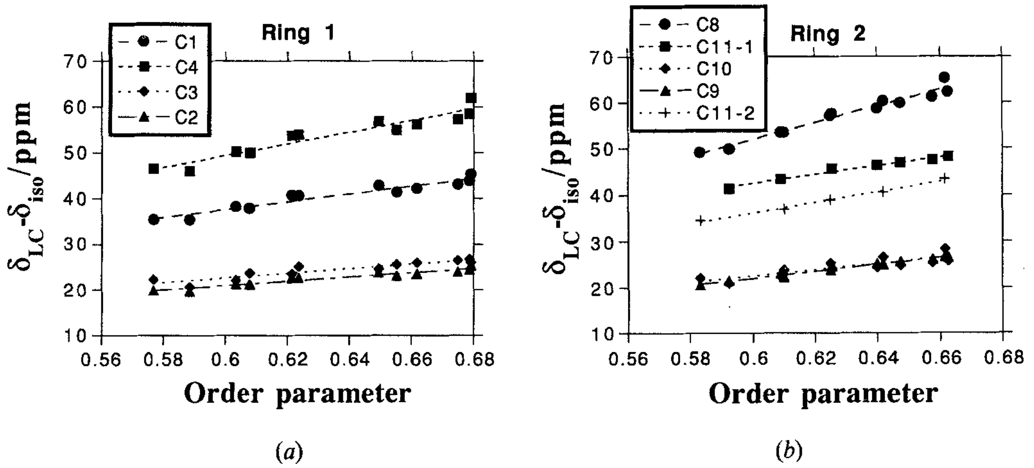

Figure 5. Linear correlation between $(\delta_{\mathrm{LC}}-\delta_{\mathrm{iso}})$ and the order parameters for (*a*) the phenyl ring (labelled ring 1) attached to the double bond and (*b*) the phenyl ring (labelled ring 2) attached to the ester group in Cin-6-2 and Cin-6-1.

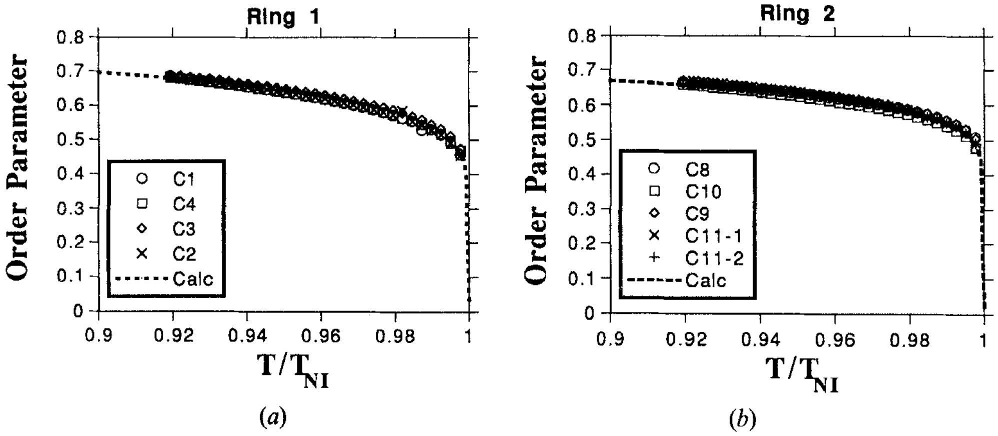

Figure 6. Order parameters calculated from equation (3) by the use of parameters determined from figure 4 as a function of the reduced temperature T/T_{NI} from the C-13 chemical shift of (*a*) the carbon atoms in ring 1 and (*b*) the carbon atoms in ring 2. The dashed lines represent the best fit of the calculated data using the empirical equation (4).

larger limiting value for the order parameter of the former is quite reasonable. The data in table 6 show that the F value for ring 2 is smaller than that for ring 1, which means that the ordering of the second ring decreases less rapidly with the increase of temperature than the ordering of the first ring. In other words, the significant difference in the values of F implies that the conformation of the mesogenic core is not independent of temperature; or, the angle between the major axis of the rigid core and the *para* axis of one or both rings is not a constant as temperature changes. Because the four-unit link is not rigid, at $T/T_{NI} \cong 1$ the wiggling motion induced by the chains would perturb the ordering of the rings differently, roughly in proportion to the length of the directly attached chain. Therefore, the cinnamic ring which is more ordered at the limit of low temperatures becomes less ordered near the clearing point due to its longer chain. The ratio between the two order parameters of ring 1 (S_{zz}) and ring 2($S_{z'z'}$) as a function of the temperature can be expressed by the formula

$$S_1/S_2 = (S_{01}/S_{02})\cdot(1 - T/T_{NI})^{F1-F2}. \qquad (4)$$

This function is plotted as a solid line in figure 7, in which the experimental ratios obtained directly by the VAS/SLF method are also presented for comparison. This

Table 6. Comparison of S_0 and F values obtained by fitting the calculated values of the order parameters to the empirical equation (4) for the two aromatic rings and for the link.

Fragment	S_0	F	Correlation coefficient
Ring 1	0·906	0·113	0·996
Ring 2	0·817	0·086	0·993
Link	0·931	0·115	0·998

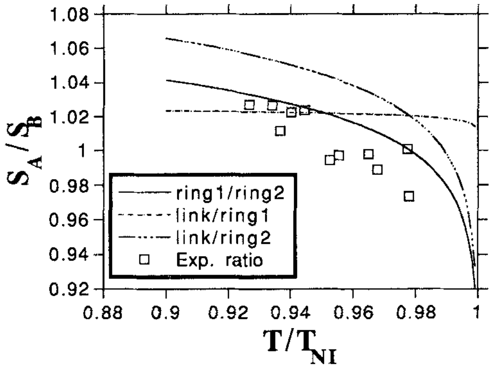

Figure 7. The ratios of the order parameter S_1/S_2 and $S_{\text{link}}/S_{\text{ring}}$ are plotted versus T/T_{NI}. The squares represent the experimental ratios obtained through the VAS/SLF method.

function and the experimental ratios show the same trends. Ring 1 is less ordered than ring 2 only above $T/T_{\text{NI}} = 0{\cdot}98$, which means that the perturbing motion of the chain is very pronounced near the clearing point. In the T/T_{NI} range studied (i.e. 0·92 to 0·98), the ratio S_1/S_2 changes from 1·03 to 1·00. This ratio is affected by the change in the geometry of each fragment which would cause a change in the major axis of the rigid core with respect to the molecular frame. For example, if we assume that the position of the major axis is unchanged with respect to ring 1, a variation of $+1{\cdot}5°$ between the major axis of the rigid core and the *para* axis of ring 2 will change the ratio S_1/S_2 from 1·00 to 1·01.

3.3. *Order parameters of the major axis of the rigid core*

In figure 4, the Z_{m} axis represents the major axis of the rigid core, so the order parameter S_{ZZ} will be defined in this frame. The order parameters S_{zz} and $S_{z'z'}$ of the two aromatic rings in their own molecular frames are related to S_{ZZ} assuming that the Z axis is uniaxial in the nematic phase

$$S_{zz} = S_{ZZ}(3\cos^2\alpha - 1)/2, \qquad (5\,a)$$

$$S_{z'z'} = S_{ZZ}(3\cos^2\alpha' - 1)/2, \qquad (5\,b)$$

where α, α' are the angles between Z_{m} and z, z', respectively. If the geometry of the linkage is known, we can expect to obtain the molecular order parameter from the dipolar couplings of the link. Then, the position of the major axis can be determined from equation (5).

Several crystal structures of cinnamic acids or cinnamic acid derivatives are known. For 4″-nitrophenyl-4′-(4′-*n*-hexyloxybenzoyloxy)-cinnamate, the ethylenic group is not co-planar with the phenyl ring to which it is attached [22]. This may be due to intramolecular forces in the pair-wise crystal packing [22], which would diminish in the liquid crystalline phase. For example, the dihedral angle between the two phenyl rings in a cyanobiphenyl crystal [23] is significantly reduced in the liquid crystalline phase [24]. If there is no special crystal packing, the ethylenic group and the attached phenyl ring are co-planar or early co-planar, as in the cases of four 4-alkoxycinnamic acids and two cinnamic acid derivatives [25–28]. This induces a bond deformation in the ethylenic linkage. From the crystallographic data of these compounds, we can deduce an average geometry defined as $d_{C4-C5}=0{\cdot}1464$ nm, $d_{C5-C6}=0{\cdot}1324$ nm, $d_{C6-C7}=0{\cdot}1453$ nm, C4–C5–C6 = 127·6°, and C5–C6–C7 = 122·4°. In other words, this average geometry is characterised by a larger C4–C5–C6 bond angle compared with the C5–C6–C7 bond angle due to steric repulsion between H3 and H6.

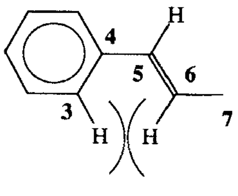

In the nematic phase, the dipolar couplings for C5–H5 and C6–H6 are quite different. The ratio of these two dipolar couplings D(C6–H6)/D(C5–H5) is essentially independent of the substituent at C11 and of the temperature, and is equal to $1{\cdot}24\pm0{\cdot}02$. This result mean that in the nematic phase, these two C–H bonds are not parallel, and that the angle between the C–H bond and the major axis of the rigid core is larger for H6 than for H5. This clearly indicates that even if the phenyl ring is rotating quite freely around the *para* axis, the steric hindrance between H6 and the *ortho* hydrogens in ring 1 causes the geometry to be quite similar to that in the solid phase with planar configuration. Therefore, we have chosen the solid state structural data for our order parameter calculations. If we take the Z axis parallel to the major axis of the rigid core axis, the X axis in the ethylenic plane and the Y axis perpendicular to this plane, the observed dipolar couplings can be expressed as

$$D_{ij}=-[\gamma_i\gamma_j h/(4\pi^2 r_{ij}^3)][(S_{ZZ}(3\cos^2\Phi_{ijZ}-1)/2+(S_{XX}\text{-}S_{YY})(\cos^2\Phi_{ijX})/2$$
$$+S_{XZ}(\cos\Phi_{ijX}\cos\Phi_{ijZ})] \qquad (6)$$

where S_{ZZ} is now the molecular order parameter as this fragment is only affected by the overall reorientation of the molecule, and Φ_{ijM} is the angle between the C_iH_i pair and the Z axis (see figure 4).

We have now six unknowns: two C–C–H angles, three order parameters and the major axis position. Unfortunately, among the six dipolar couplings, four are not very accurate because they are relatively small. Due to the *trans* geometry, the coupling between the protonated carbon and the bonded proton is nearly half the value obtained with a *cis* geometry. Therefore, we have used the values of S_{zz} determined above and equation (5 *a*) as an additional constraint in order to gain more accuracy in the least squares calculations. The calculated value of the angle C5–C6–H6 is essentially the same for the two compounds at different temperatures, and the average value of 120·3°±0·5° was taken as a constant to refine the calculation. The results are listed in table 7. The value of 115·1° for the C6–C5–H5 angle is consistent with the high value of 126·7° for the C4–C5–C6 angle. The difference of 5° between the two C–H bonds cannot be explained without taking into account the steric hindrance between H6 and the *ortho* hydrogens in ring 1. The $S_{xx}-S_{yy}$ value is of the same order of magnitude compared with the corresponding one for the aromatic ring. The angle α between the major axis of the rigid core and the symmetry axis of the first ring is quite small, and it is consistent with the assumption that the major axis position should be closely related to the axis of

Table 7. Structural and order parameters for the ethylenic link obtained from the dipolar couplings. The data are average values for 0·92 < T/T_{NI} < 0·98 because the results do not show systematic dependence on temperature.

C6–C5–H5	S_{XZ}	$S_{XX}-S_{YY}$	α
115·1° ± 0·5	−0·14 ± 0·02	0·074 ± 0·015	4·0° ± 0·9°

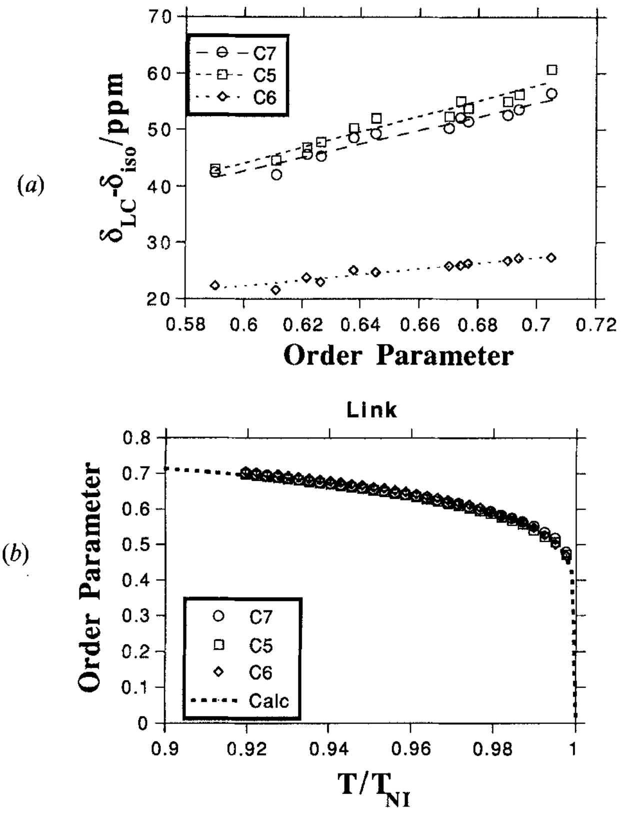

Figure 8. (*a*) Linear correlation between ($\delta_{LC}-\delta_{iso}$) and the experimental order parameters for the link. (*b*) Order parameters calculated from equation (3) by the use of parameters determined from (*a*) as a function of the reduced temperature T/T_{NI} from the C-13 chemical shift of the three carbon atoms in the link. The dashed lines represent the best fit of the calculated data using the empirical equation (3).

maximum order for the different fragments [29]. On average, the angle, α, seems to be slightly less for Cin-6-1 than for Cin-6-2, but the difference is within the range of the uncertainty.

Assuming that the only temperature dependent term is S_{ZZ}, we can use the empirical formula (2) to relate the anisotropic chemical shift to the order parameter, S_{ZZ}. This linear relationship is verified by the data shown in figure 8 (*a*). From the *a* and *b* values obtained for each carbon, values of S_{ZZ} in a more extended temperature range can be calculated from the chemical shifts. Then, these data can be fitted using the empirical formula (3) as shown in figure 8 (*b*). The values of S_0 and F are given in table 6 along with those for the phenyl rings. As expected, the limiting value S_0 is slightly higher than that for ring 1. More surprisingly, the two F values are very similar which means that the temperature dependence of the order parameters for ring 1 and for the link is almost the same. The nearly constant ratio of $S_{\mathrm{link}}/S_{\mathrm{ring}}$ for ring 1, shown in figure 7, means that the angle, α, between the *para* axis of ring 1 and the major axis of the rigid core remains essentially unchanged. On the contrary, the angle, α', between the *para* axis of ring 2 and the major axis of the rigid core position changes with temperature and this angle is 7° at T/T_{NI}-0·98 and 11° at $T/T_{\mathrm{NI}}=0{\cdot}92$. This is quite understandable if we recall that the double bond is strongly conjugated with ring 1 but is connected to ring 2 via the more flexible carboxyl group.

3.4. *C–H order parameters of the chains*

For the alkoxy chain, the observed dipolar couplings represent the weighted average orientation of each C–H bond. Due to the approximate cylindrical symmetry of the C–H bond, the order parameter is directly proportional to the C–H dipolar coupling as [3]

$$S_{\mathrm{C\text{-}H}} = -4{\cdot}407\times 10^{-5} D_{\mathrm{C\text{-}H}}. \qquad (7)$$

The order parameters for various aliphatic carbon atoms in Cin-6-2 are plotted in figure 9 in which the well-known odd-even effect is quite evident. Because of this effect, $S_{\mathrm{C-H}}$ for the terminal methyl group in the alkyl chain is close to zero when the number of atoms in the chain is even, as in the compounds studied here, but its $S_{\mathrm{C-H}}$ is rather appreciable when the number of atoms in the alkoxy chain is odd. It has been shown that equation (2) is applicable for the aliphatic carbons in cyanobiphenyls [14]. The data plotted in figure 10 show that this is also true for the cinnamates studied here.

4. Conclusions

In conclusion, a combination of 2D VAS/SLF results in conjunction with the anisotropic chemical shift measurements from one dimensional experiments gives a simple and accurate way to obtain the dependence of the order parameter as a function of reduced temperature. This dependence can be found for every fragment of the molecule. Because the four-unit link –CH=CH–COO– is not rigid and

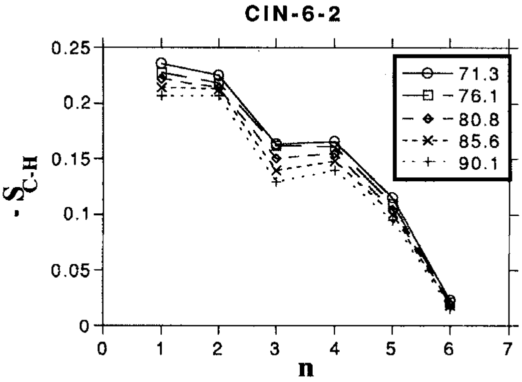

Figure 9. The values of $-S_{\mathrm{C-H}}$ for the alkoxy chain in cin-6-2 at five temperatures.

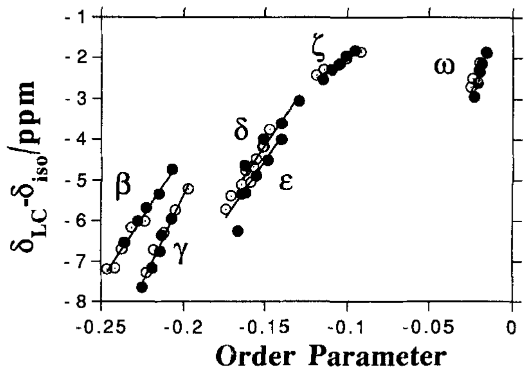

Figure 10. Linear correlation between ($\delta_{LC}-\delta_{iso}$) and the order parameters for the aliphatic carbons in the alkoxy chain. ○ and ● represent the experiment points for Cin-6-1 and Cin-6-2, respectively.

because one terminal chain is short, the ordering behaviour of the two phenyl rings depends on the reduced temperature differently. Near the N–I transition the ordering is governed by the length of the terminal chain, and the ring bearing the shortest chain is the most ordered. Far from the transition temperature the difference in the ordering is governed by the extent of conjugation; the ring bearing the double bond is more conjugated and more ordered than the one bearing the carboxyl group. As a consequence, the average geometry of the mesogen and the major axis of the rigid core in the molecular frame can change slightly with temperature. By comparison between the ordering parameters of the different fragments, we have shown that the position of the major axis of the rigid core with respect to the phenyl ring connected to the ethylenic group is unchanged with temperature but the angle between the major axis of the rigid core and the *para* axis of the phenyl ring connected to the carboxylic group is temperature dependent.

The authors acknowledge financial support by NATO (to J. P. Bayle) and the U.S. National Science Foundation (grant No. DMR-9018753 to B. M. Fung), and the technical assistance of Dr W. Guo.

References

[1] Emsley, J. W. (editor), 1985, *Nuclear Magnetic Resonances of Liquid Crystals* (Reidel).
[2] Fung, B. M., and Afzal, J., 1986, *J. Am. chem. Soc.*, **108,** 1107.
[3] Fung, B. M., Afzal, J., Foss, T., and Chau, M.-H., 1986, *J. chem. Phys.*, **85,** 4808.
[4] Fung, B. M., Poon, C. D., Gangoda, M., Enwall, E. L., Diep, T. A. D., and Bui, C., 1986, *Molec. Crystals liq. Crystals*, **141,** 267.
[5] Poon, C. D., Wooldridge, C. M., and Fung, B. M., 1988, *Molec. Crystals liq. Crystals*, **157,** 303.
[6] Foster, P., and Fung, B. M., 1988, *J. chem. Soc. Faraday Trans. II*, **84,** 1083.
[7] Frech, C. B., Fung, B. M., and Schadt, M., 1988, *Liq. Crystals*, **3,** 713.
[8] Frech, C. B., Fung, B. M., and Schadt, M., 1989, *SPIE Proc.*, **1080,** 215.
[9] Poon, C. D., and Fung, B. M., 1989, *Liq. Crystals*, **5,** 1159.
[10] Poon, C. D., and Fung, B. M., 1989, *J. chem. Phys.*, **91,** 7392.
[11] Richter, W., Fung, B. M., and Schadt, M., 1990, *Liq. Crystals*, **8,** 63.
[12] Richter, W., Reimer, D., Fung, B. M., Twieg, R. J., and Betterton, K., 1990, *Liq. Crystals*, **8,** 687.
[13] Guo, W., and Fung, B. M., 1991, *Liq. Crystals*, **9,** 117.

[14] Guo, W., and Fung, B. M., 1991, *J. chem. Phys.*, **95**, 3917.

[15] Balakrishnan, N. S., Bayle, J. P., Ho, M.-S., Pham, S. C., and Fung, B. M., *Liq. Crystals*, **14**, 591.

[16] Fung, B. M., Magnuson, M. L., Tong, T.-H., and Ho, M.-S., 1993, *Liq. Crystals*, **14**, 1495.

[17] Berdagué, P., Perez F., Courtieu J., and Bayle, J. P., 1993, *Bull. Soc. chim. Fr.* (in the press). See also Vogel, A., 1989, *Textbook of Practical Organic Chemistry* (Lohgman Scientific and Technical), p. 1038.

[18] Leslie, T. M., 1984, *Ferroelectrics*, **58**, 9.

[19] Dave, J. S., and Lohar, J. M., 1989, *J. Indian chem. Soc.*, **66**, 25.

[20] Mehring, M., 1983, *High Resolution NMR in Solids* (Springer-Verlag), p. 253.

[21] Haller, I., 1975, *Prog. Solid St. Chem.*, **10**, 103.

[22] Gehring, S., Fan, Z. X., Haase, W., Muller, H., and Gallardo, H., 1989, *Molec. Crystals liq. Crystals*, **168**, 125.

[23] Haase, W., Paulus, H., and Pendzialek, R., 1983, *Molec. Crystals liq. Crystals*, **100**, 211.

[24] Sinton, S. W., Zax, D. B., Murdoch, J. B., and Pines, A., 1984, *Molec. Phys.*, **53**, 333.

[25] Bryan, R. F., and Forcier, P. G., 1980, *Molec. Crystals liq. Crystals*, **60**, 157.

[26] Bryan, R. F., and Hartley, P., 1981, *Molec. Crystals liq. Crystals*, **69**, 47.

[27] Huber, C. P., 1985, *Acta crystallogr.*, **C41**, 1076.

[28] Rabinovich, D., 1969, *J. chem. Soc.* A, 2361.

[29] Catalano, D., Forte, C., Veracini, C. A., Emsley, J. W., and Shilstone, G. N., 1987, *Liq. Crystals*, **2**, 345.